

Dual Tweezer Behavior of an Octapodal Pyrene Porphyrin-based System as a Host for Fullerenes

Sergio Ferrero, Héctor Barbero, Daniel Miguel, Raúl García-Rodríguez* and Celedonio M. Álvarez*

GIR MIOMeT, IU CINQUIMA/Química Inorgánica, Facultad de Ciencias, Universidad de Valladolid, E-47011, Valladolid, Spain

Supporting Information Placeholder

ABSTRACT: The incorporation of eight pyrene units in a single porphyrin core exhibits a great synergistic effect, resulting in high affinity towards C_{60} and C_{70} . This octapyrene porphyrin is easily accessible by a straightforward two-step synthetic approach that involves an octuple Suzuki reaction. The new supramolecular platform can present single or double tweezer fullerene hosting behavior. The switch from double to single tweezer behaviour is triggered by the simple coordination of Zn^{2+} to the porphyrin. Both the octa-pyrene porphyrin **2HPOP** and its zinc metalloporphyrin analogue **ZnPOP** show very high affinity for C_{60} and C_{70} , while simultaneously allowing the discrimination of C_{70} over C_{60} in a C_{60}/C_{70} mixture. The use of **2HPOP** and **ZnPOP** for the enrichment of real fullerene mixtures is also demonstrated.

INTRODUCTION

Intermolecular π - π interactions are one of the main driving forces responsible for controlling supramolecular chemistry in carbon nanostructures.¹ In this regard, shape complementarity between the different nanostructures is known to play a major role. It is also widely accepted that good interaction with C_{60} or C_{70} requires non-planar structures,² and in this context non-planar polycyclic aromatic hydrocarbons (PAHs), such as the unique bowl-shaped corannulene-based systems, have emerged as very important.³ On the other hand, systems based on the planar PAH pyrene are ideally suited for interaction with more extended structures such as carbon nanotubes⁴ and graphene.⁵ Not surprisingly, only a few examples of pyrene-fullerene interactions have been reported,⁶ most of them involving the design of complex molecular cages.⁷ In contrast with non-planar PAH-based approaches,⁸ no discrimination between C_{60} and C_{70} has been reported for pyrene-based systems. This is quite surprising, since current supramolecular approaches require more complex scaffolds based on non-planar PAHs such as corannulene moieties⁹ which are not easily synthetically accessible. Achieving a good balance between facile synthesis and a high affinity constant, and in particular the ability to achieve discrimination, still remains challenging. Therefore, the development of cheaper and more synthetically accessible pyrene-based systems is an attractive but difficult task.

In the search for new molecular architectures that act as hosts for fullerenes, researchers have focused on porphyrin-based systems. Although porphyrins are known to interact with fullerenes and co-crystallization adducts have been extensively reported,¹⁰

for a single core porphyrin, this interaction is usually too weak to be observed in solution.^{10a, 10c, 11} Therefore, in order to achieve high affinity constants, the preparation of multiporphyrinic cages is required.¹² Considerable efforts have been devoted to the tailoring of such complex systems to improve the interaction with fullerenes. Although this approach has been shown to provide some remarkably high affinities towards fullerenes, including selectivity for C₇₀ over C₆₀,^{11a, 12-13} their complex, multistep, and tedious syntheses prevent this approach from becoming general for fullerene interaction and discrimination. We have recently shown that easily accessible porphyrins based on a meso-substituted tetraaryl porphyrin core bearing different PAH units could be used for C₆₀ hosting.¹⁴ The corannulene-based system, which contained four corannulene units, showed a remarkably high affinity constant ($K_a = 2.2 \times 10^4 \text{ M}^{-1}$) for the α_4 atropisomer, presenting a 1:1 binding stoichiometry. One distinct limitation, however, was that the formation of atropisomers, whose separation was not possible, not only resulted in a complex and difficult-to-analyse mixture of species, but also diminished the interaction with C₆₀.

Herein, we report the first example of a single core porphyrin that discriminates C₇₀ over C₆₀ in a fullerene mixture. The system is based on the simultaneous introduction of eight commercially available planar PAH pyrene moieties at the meta positions on a tetraaryl porphyrin system. This not only avoids the formation of atropisomers, but also results in a great synergistic effect between the porphyrin core and the pyrene units (Figure 1). This approach avoids the use of less synthetically and commercially accessible systems, such as those based on non-planar PAHs like corannulene, and also introduces the possibility for the system to act as a single or a double-tweezer structure as a host for fullerenes. This particular behaviour stems from the arrangement of four pyrene arms above and four below the porphyrin ring plane, resulting in a ‘double picket fence’ porphyrin.

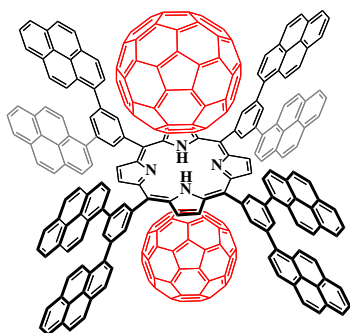


Figure 1. Idealized schematic representation of the tetraaryl octapyrene porphyrin reported in this work and its potential behavior as a double-tweezer structure to host fullerenes.

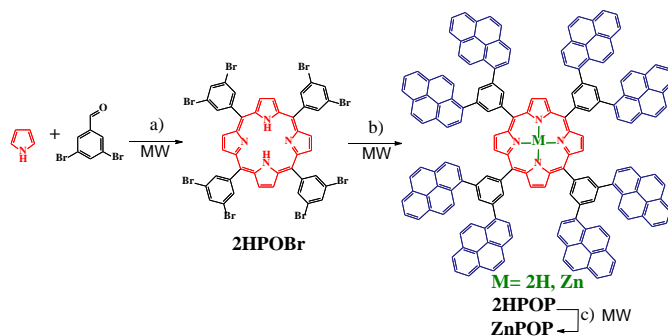
RESULTS AND DISCUSSION

As noted in the introduction, porphyrin systems are ideal scaffolds for constructing relatively complex molecular architectures. Although one unit of pyrene is known not to affect the recognition of fullerenes, we reasoned that fullerene recognition could be achieved through the cooperative effect of several units of pyrene on a porphyrin core. We sought to introduce two pyrene moieties at the meta position of an aryl group of a symmetrically substituted meso tetraaryl porphyrin to yield an octapyrene-based system (Figure 1). In such a system, the formation of atropisomers is prevented and the pyrene units would be ideally placed to

interact with fullerenes in a cooperative manner thanks to the particular arrangement provided by the central scaffold. This, along with the great synergistic effect between the porphyrin core and the pyrene units, would result in a simple but effective platform for fullerene hosting. In addition to this, the 4+4 arrangement of the pyrene arms in the “up” and “down” positions with regards to the porphyrin plane could allow the system to act as a double molecular tweezer for which 1:2 supramolecular interactions could occur.

We envisaged that such a system could be easily prepared in a two-step synthesis following the so-called “divergent” approach, in which a suitable porphyrin core with functionalities that can be subsequently used as reactive points for the construction of a more complex scaffold is first prepared. Our initial attempts involving the reaction of the meta-substituted octaboronate-porphyrin compound **2HPOB** and 1-bromopyrene resulted in an extremely low yield (less than 1%) for the octa Suzuki reaction (see SI, route 2). However, this could be easily circumvented by employing the meta substituted octabromo-porphyrin **2HPOBr** as the starting porphyrin core (Scheme 1). The synthesis of this compound was easily accomplished in 15 min by a MW-assisted method in which **2HPOBr** cleanly precipitates from the reaction mixture (see experimental section). This approach drastically improved the yield (24%) compared to that of the previously existing method (11%), which required of 48 h of reflux in propionic acid and purification by chromatography.¹⁵ With this compound in hand, the target compound **2HPOP** was obtained via a MW-assisted octuple Suzuki reaction. The use of a MW reactor is critical for the success of the reaction, as it is known to drastically decrease the amount of undesired byproducts.¹⁶ This can be easily realised from the remarkably high total yield of 28% (i.e., more than 85% per single cross-coupling reaction) and the fact that similar reactions involving a high number of Pd-catalysed C-C couplings are known to be problematic due to the rapid build-up of by-products, which can completely prevent product formation.¹⁷ Metallation of **2HPOP** with $\text{Zn}(\text{OAc})_2 \cdot 2\text{H}_2\text{O}$ to give **ZnPOP** (Scheme 1) was straightforwardly achieved in a quantitative manner, thus providing an additional platform for fullerene hosting and also for evaluating the impact of the introduction of a metal on the supramolecular binding behaviour. It is known that metal insertion can lead to remarkable changes in the geometry of the central ring of the porphyrin¹⁸ and provide a new set of noncovalent interactions^{10a, 11a, 19}, both of which may lead to a change in the hosting behaviour of the system.

Scheme 1 Optimized synthesis of **2HPOP** and **ZnPOP**^a



^aReagents and conditions: (a) propionic acid, nitrobenzene, MW, 200 °C; (b) Bpin-Pyrene (**1**), $[\text{PdCl}_2(\text{dppf})]$, ^tBuONa, toluene, MW, (c) $\text{Zn}(\text{OAc})_2 \cdot 2\text{H}_2\text{O}$, $\text{CHCl}_3/\text{toluene}$, MW, 120 °C.

All the aforementioned porphyrins were fully characterized by NMR spectroscopy, UV-Vis absorption spectroscopy and high-resolution MALDI-TOF mass spectrometry (see the experimental part and SI). The UV-Vis absorption spectra in toluene display the expected weak Q-bands in the range 500-670 nm and the intense Soret bands, which are red-shifted for **ZnPOP** (432 nm) as compared to **2HPOP** (428 nm). This small but distinctive red-shift of the band has been suggested to be related to an increase in the non-planarity of the porphyrin.^{18d, 20} ¹H NMR spectra of the octapyrene porphyrins **2HPOP** and **ZnPOP** show the equivalency of the eight pyrene moieties resulting from the effective D_{4h} symmetry in solution (see ¹H and ¹³C{¹H} spectra in the SI). The presence of the two inner NH protons of **2HPOP** is observed at a characteristic upfield shift of $\delta = -2.50$ ppm as a consequence of the shielding they experience from the aromatic ring current present in the porphyrin core. This signal is absent in the metallated porphyrin **ZnPOP**. It is worth mentioning the different behavior observed for **2HPOP** and **ZnPOP** in CDCl₃. While the ¹H NMR spectrum of **2HPOP** exhibits sharp resonances for the range of concentrations studied (10⁻⁴-10⁻⁶ M), **ZnPOP** shows very broad resonances in relatively dilute solutions (10⁻⁵ M) that become sharper with the further dilution of the sample (See SI, Figs S9). This behavior is indicative of an intermolecular process.²¹ However, both **2HPOP** and **ZnPOP** show non-concentration-dependent behavior in toluene-d₈, a solvent that is known to disrupt intermolecular π - π stacking interactions.^{10a, 21a} This suggests that **ZnPOP**, unlike its unmetallated analogue **2HPOP**, may undergo a certain degree of stacking due to π - π interactions between porphyrins in CDCl₃. The extent to which the Zn centre directly contributes to the formation of these π - π stacking interactions is unknown at this stage.

We then moved to study the supramolecular behavior of **ZnPOP** and **2HPOP** as hosts for C₆₀ and C₇₀. We were particularly interested in studying whether these porphyrin systems could act as a single or double tweezers (i.e., whether they could accept one or two fullerenes, as shown in Fig. 1). We initially used a host concentration of [H]₀ = 10⁻⁴ M. Although the titrations could be carried out for C₆₀, the titration of **ZnPOP** and **2HPOP** with C₇₀ was prevented by the appearance of a precipitate. This suggested a much larger affinity of both systems for C₇₀ than for C₆₀, for which no precipitate was observed. We therefore set the concentration of host to [H]₀ = 10⁻⁵ M for the titration experiments involving C₇₀. We started our studies with **ZnPOP**, and we carried out titration experiments with C₆₀ and C₇₀ in toluene-d₈. In both experiments, we followed the shift of H₈ (see figure 2, S22 and S24 in the SI) during the titration. As shown in Figure 2 above, the chemical shift for H₈ changes during the titration of **ZnPOP** with C₆₀ or C₇₀, indicating supramolecular association and host-guest formation in both cases. The non-linear binding isotherm that results from the titration experiments with C₆₀ or C₇₀ could be fitted, in both cases, to a 1:1 model (Fig. 2 below). No evidence for a 1:2 model in which **ZnPOP** accepts two fullerenes was observed. These plots clearly show a faster saturation for C₇₀, which reaches the limiting chemical shift $\Delta\delta_{\max}$ much faster than C₆₀, reflecting a greater binding constant value K_a for **ZnPOP** and C₇₀. The calculated binding constants of **ZnPOP** for C₆₀ and C₇₀ are K₁ = 2.30±0.01x10³ M⁻¹ and K₁ = 2.69±0.02x10⁴ M⁻¹, respectively. This shows that **ZnPOP** has a very high selectivity, preferring C₇₀ over C₆₀, as demonstrated by the binding constant for C₇₀, which is an order of magnitude larger than the one for C₆₀.

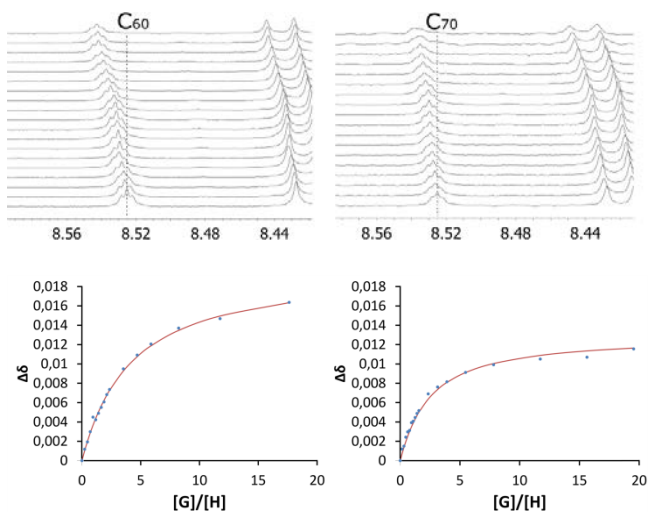


Figure 2. (Above) ¹H NMR spectra in toluene-d₈ showing the H₈ chemical shift of **ZnPOP** upon the addition of aliquots of C₆₀ (left) or C₇₀ (right). (Below). Plot of the changes in the chemical shift against [G]/[H], where G (guest) is C₆₀ or C₇₀ and H (host) is **ZnPOP**. The red line corresponds to the nonlinear fitting of Δδ for H₈ to a 1:1 binding isotherm. It can be seen that the titration with C₇₀ reaches supra-molecular saturation earlier than C₆₀, reflecting a larger binding constant. Note: [H]₀ = 10⁻⁴ M for C₆₀ titration and [H]₀ = 10⁻⁵ M for C₇₀.

In sharp contrast, the titration of **2HPOP** with C₇₀ did not show the typical 1:1 binding isotherm observed for **ZnPOP**. Instead, a very complex behaviour was observed, indicative of a non-1:1 system.²² This complex behaviour was observed at different initial concentrations of the host, [H]₀ (see figure S28 and S30 SI). Figure 3 shows the change of Δδ against [Guest]/[Host]. The graph shows two inflexion points at [G]/[H] = 1 and *ca.* [G]/[H] = 2. The binding isotherm could be fitted to a 1:2 non-cooperative model for which the values $K_1 = 1.40 \pm 0.05 \times 10^4 \text{ M}^{-1}$ and $K_2 = 3.50 \pm 0.13 \times 10^3 \text{ M}^{-1}$ were obtained.²³ This double tweezer behaviour of **2HPOP** was also observed for the interaction with C₆₀. The binding isotherm observed in this case did not show such complex behaviour, but instead an asymptotic curve. This apparently simple behaviour could also be better explained by a 1:2 non-cooperative model (cov_{fit} = 3.16)^{23b} with $K_1 = 1.49 \pm 0.01 \times 10^3 \text{ M}^{-1}$ and $K_2 = 3.71 \pm 0.02 \times 10^2 \text{ M}^{-1}$ (see SI for details), than by a 1:1 model as in the case of **ZnPOP**.

These results show that the selection between double/single tweezer behavior might be controlled by simply coordinating Zn²⁺ in the porphyrin, thus illustrating how subtle changes in the porphyrin skeleton may lead to drastic changes in their supramolecular behavior.

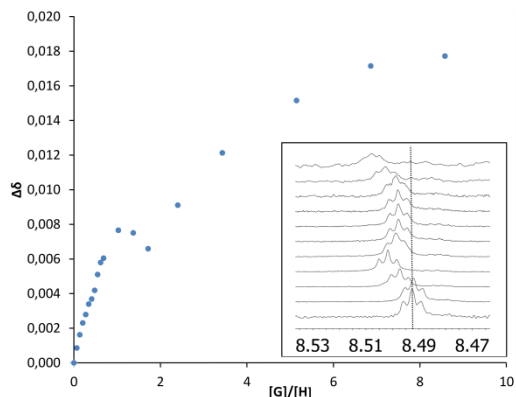


Figure 3. Plot of changes in the chemical shift of H_8 against $[G]/[H]$, where G (guest) is C_{70} and H (host) is **2HPOP**, showing the more complex behaviour of the binding isotherm. $[H]_0 = 10^{-5}$ M. Inset, stacked 1H NMR spectra showing the variation of the H_8 chemical shift of **2HPOP**, $[H]_0 = 10^{-4}$ M, upon the addition of aliquots of C_{70} . Note: the dotted line is a guide to the eye.

Importantly, the great selectivity for C_{70} over C_{60} (one order of magnitude) is retained in the case of **2HPOP** when switching from a single tweezer behaviour, as observed in **ZnPOP**, to a double tweezer one (Table 1). It is worth mentioning that the binding constants for both fullerenes are similar to those based on non-planar PAH systems bearing more complex corannulene motifs, whose bowl-shaped polycyclic aromatic hydrocarbon structure is known to provide complementarity between corannulene-fullerene surfaces.^{8b, 24} For instance, Sygula's buckycatcher with two corannulene pincers on a cyclooctatetraene framework presented associations of $(3.20 \pm 15) \times 10^3 M^{-1}$ for C_{60} and $(4.60 \pm 17) \times 10^3 M^{-1}$ for C_{70} (toluene, 298K),^{9a, 9c} and our platinum based molecular tweezer with two corannulene units presented associations of $(2.07 \pm 6) \times 10^3 M^{-1}$ for C_{60} and $(4.60 \pm 1) \times 10^4 M^{-1}$ for C_{70} , the highest at the time for a corannulene based system (toluene, 298K).^{8a} As discussed in the introduction, our previously reported tetraaryl porphyrin core bearing four corannulene units in the para position showed a remarkably high affinity for C_{60} for its α_4 atropisomer $2.2 \times 10^4 M^{-1}$ (toluene, 298K). However the formation of atropisomers drastically decreased the overall association ability of the system.¹⁴ This shows the great potential of our simple approach based on the two-step synthesis of a single porphyrin bearing eight pyrene units.

Table 1. Summary of Binding Constants K_a (M^{-1}) of **2HPOP** and **ZnPOP** for C_{60} ($[H]_0 = 10^{-4}$ M) and C_{70} ($[H]_0 = 10^{-5}$ M) in Toluene- d_8

	C_{60}	C_{70}
ZnPOP	$K_1 = 2.30 \pm 0.01 \times 10^3$	$K_1 = 2.69 \pm 0.02 \times 10^4$
2HPOP	$K_1 = 1.49 \pm 0.01 \times 10^3$ $K_2 = 3.71 \pm 0.02 \times 10^2$	$K_1 = 1.40 \pm 0.05 \times 10^4$ $K_2 = 3.50 \pm 0.13 \times 10^3$

Having established that the switch from double to single tweezer behaviour is triggered by the simple coordination of Zn^{2+} to the porphyrin core, we then moved to evaluate the possibility of using these systems to separate/enrich a C_{60}/C_{70} fullerene mixture by selectively sequestering C_{70} from the solution. We were motivated to explore this possibility by the large selectivity for C_{70}

over C_{60} shown by **ZnPOP** and **2HPOP**, as well as the low solubility of the adducts formed with C_{70} , as noted above. We initially dissolved an equimolar amount of C_{60}/C_{70} in toluene- d_8 and recorded a $^{13}C\{^1H\}$ NMR spectrum²⁵ (Figure 4, above). The addition of one equivalent of **2HPOP** resulted in the formation of the fullerene-porphyrin adduct as a black precipitate after sonication of the sample, which could be easily separated from the supernatant by simply decanting the solution. The $^{13}C\{^1H\}$ spectrum of the decanted supernatant shows a C_{70}/C_{60} ratio of 1:2.7 (Figure 4, below), which was also verified by UV-Vis and HPLC.^{25b, 26} Thus, a nearly three times more enriched sample of C_{60} was easily obtained by simply adding one equivalent of **2HPOP**. The level of enrichment of C_{60} in solution was found to increase steadily with the addition of **2HPOP**. The addition of 0.7 eq and 1.6 eq to 1:1 mixtures of C_{70}/C_{60} resulted in enrichment levels of 1:2.0 and 1:4.6 of C_{60} in the solution, respectively, as analyzed by $^{13}C\{^1H\}$ NMR, UV-Vis and HPLC, with a loss of 42% of C_{60} as co-precipitate for the latter case (see SI).

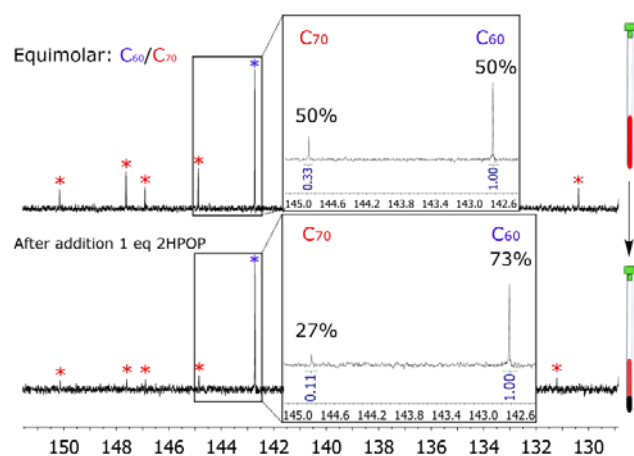


Figure 4. Quantitative $^{13}C\{^1H\}$ NMR spectra in toluene- d_8 of an equimolar solution of C_{60}/C_{70} before (above) and after (below) the addition of 1 equivalent of **2HPOP**. Signals of C_{70} are reduced as a result of its precipitation as the **2HPOP** adduct of C_{70} . Note: The 5 resonances for C_{70} are shown with red asterisks, and the one for C_{60} with a purple asterisk. The fullerene C_{60}/C_{70} ratio was extracted from the integration of their signals considering their relative proportion of nuclei.

Encouraged by these good results, we turned our attention towards the use of **ZnPOP** for fullerene enrichment. We were intrigued to test whether we could improve the results obtained with **2HPOP** and minimise the amount of C_{60} loss as co-precipitate. We found that the addition of 1 equivalent of **ZnPOP** to a 1:1 mixture of C_{70}/C_{60} in toluene resulted in a 1:8.1 enrichment of C_{60} in solution, while only losing 13% of the initial amount of C_{60} by co-precipitation, thus improving the results obtained with **2HPOP**. A distinctive difference in this case is that **ZnPOP** behaves as a single tweezer for fullerene recognition, while in the case of **2HPOP** the loss of C_{60} as co-precipitate could be enhanced by its double tweezer behaviour. These results are still far from the best ones obtained with carefully designed porphyrin-based molecular cages.²⁷ For example, Zhang et al designed a 3-D rectangular prismatic molecular cage displaying an astonishingly high separation of C_{70} from a C_{60} -enriched fullerene mixture, with a 9-fold increase in the separation of C_{70} from a C_{60} -enriched fullerene mixture (from 9 mol% to 79

mol%).^{27a} Nonetheless, our results show the generality of this approach to enrich fullerene mixtures in a simple and handy manner.

CONCLUSIONS

We have reported a two-step synthesis of a single porphyrin core system bearing 8 pyrene units that shows high affinity towards C₆₀ and C₇₀. The key to the success of our approach is the integration of 8 pyrene units in a tetraaryl meso-substituted porphyrin, which results in a great synergistic effect between the porphyrin core and the pyrene units. The resulting ‘double picket fence’ porphyrin can behave as either a double or single tweezer simply by the introduction of Zn²⁺ into the porphyrin core, which triggers the switch from double (**2HPOP**) to single (**ZnPOP**) tweezer behavior, thus allowing additional control of our supramolecular platform. In addition to this, **ZnPOP** and **2HPOP** can discriminate between C₇₀ and C₆₀, and their use for the easy enrichment of C₆₀/C₇₀ mixtures of fullerenes is demonstrated. To the best of our knowledge, this constitutes the first example of discrimination between C₆₀ and C₇₀ using a pyrene-based molecular tweezer. This type of discrimination has generally been the domain of non-planar PAH systems that display greater shape complementarity or of complex molecular cages, but both designs are much more synthetically costly. Ongoing research in our labs is aimed at developing new octapodal non-planar PAH porphyrin-based systems for fullerene discrimination, as well as probing the exact mechanism of the single and double tweezer behaviour in these new and fascinating supramolecular systems.

EXPERIMENTAL

General Methods

All reagents were purchased from commercial sources and used without further purification. Solvents were either used as purchased or dried according to procedures described elsewhere.²⁸ Microwave reactions were carried out using an Anton Paar Monowave 300 Reactor. Column chromatography was carried out using silica gel 60 (particle size 0.040–0.063 mm; 230–400 mesh) as the stationary phase, and TLC was performed on precoated silica gel plates (0.25 mm thick, 60 F254) and visualized under UV light and/or by immersion in anisaldehyde. NMR spectra and NMR titrations were recorded on 500 MHz Agilent DD2 instruments equipped with a coldprobe in the Laboratory of Instrumental Techniques (LTI) Research Facilities, University of Valladolid. Fullerene ¹³C{¹H} NMR experiments were recorded on 500 MHz Agilent instruments equipped with a ONEPROBE using the following acquisition parameters: 4 s relaxation delay between transients, 45° pulse width, and 1.048 s acquisition time. ¹H and ¹³C NMR chemical shifts (δ) are reported in parts per million (ppm) and are referenced to TMS, using the solvent as an internal reference. Coupling constants (*J*) are reported in Hz. Standard abbreviations are used to indicate multiplicity: s = singlet, d = doublet, t = triplet, m = multiplet. ¹H and ¹³C peak assignments were performed using 2D NMR methods (DQF-COSY, band selective ¹H-¹H-ROESY, band selective ¹H-¹³C HSQC, band selective ¹H-¹³C HMBC). Due to low solubility, some carbon signals were detected indirectly via ¹H-¹³C-HMBC experiments; in these cases, the abbreviation *in* is used. High resolution mass spectra were recorded at the mass spectrometry service of the Laboratory of Instrumental Techniques (LTI) of the University of Valladolid. A MALDI-TOF system (MALDI-TOF), the Bruker Autoflex Speed (N₂ laser: 337 nm, pulse energy 100 μJ, 1 ns;

acceleration voltage: 19 kV, reflector positive mode) was used. Trans-2-[3-(4-tert-butylphenyl)-2-methyl-2-propenylidene]malonitrile (DCTB) and 1,8,9-anthracenetriol, 1,8-dihydroxy-9(10H)-anthracenone (dithranol) were used as matrices. UV/Vis spectra were recorded using a Shimadzu UV-1603 with spectrophotometric grade solvents. UV/vis absorption spectral wavelengths (λ) are reported in nanometers (nm), and molar absorption coefficients (ϵ) are reported in $\text{M}^{-1} \text{cm}^{-1}$. High performance liquid chromatography (HPLC) was performed at the chromatography service of the Laboratory of Instrumental Techniques (LTI) of the University of Valladolid using an Agilent 1200 Series with a C18 column (4.6 mm \times 250 mm) with a UV/Vis (333 nm) detector. The mobile phase was toluene/methanol/acetonitrile (60:20:20) containing 0.1% trifluoroacetic acid (TFA) at 30 °C.

Pinacol pyreneboronate (**1**)

1-pyreneboronic acid (100 mg, 0.406 mmol) and pinacol (72.3 mg, 0.609 mmol) were placed into a sealed vessel specifically designed for microwave irradiation. Initially, the mixture was heated inside a microwave reactor at 140 °C without stirring, allowing pinacol to melt, and then stirred for 15 min. The mixture was dissolved in 20 ml of DCM and placed into a separatory funnel with 20 ml of warm H₂O. The organic phase was washed with 20 ml of warm H₂O twice, and the aqueous phase was extracted with 10 ml of DCM. The organic layer was dried with anhydrous MgSO₄, filtered and concentrated to afford **1** as a pure white solid (128 mg, 96%). The spectroscopic data were in agreement with those reported in the literature.²⁹

2HPOBr

Pyrrole (139 μL , 2 mmol), 3,5-dibromobenzaldehyde (557 mg, 2 mmol), propionic acid (7 mL, 87 mmol) and nitrobenzene (13 mL, 126 mmol) were mixed in a sealed vessel specifically designed for microwave irradiation. The mixture was stirred inside a microwave reactor at 200 °C for 15 min; the pressure reached up to 4 bar. The dark crude was stored in a refrigerator for 2 days and then filtered in a Büchner funnel and washed with MeOH. The obtained solid was placed in an oven and kept under reduced pressure (200 °C, 3 h, 90 torr) to remove residual nitrobenzene and finally give the dark purple solid **2HPOBr** (150 mg, 24% yield). ¹H NMR (500 MHz, Chloroform-*d*): δ 8.89 (s, 8H, H₂), 8.31 (d, J = 1.8 Hz, 8H, H₆), 8.15 (t, J = 1.8 Hz, 4H, H₈), -2.99 (br, 2H, H₁). ¹³C{¹H} NMR (126 MHz, Chloroform-*d*): δ 144.9 (C₅), 135.9 (C₆), 133.9 (C₈), 121.6 (C₇), 117.6 (C_{4-in}). HRMS (MALDI-TOF) *m/z*: [M+H]⁺ Calcd for C₄₄H₂₂Br₈N₄ 1246.5310; Found 1246.5311 (0.1 ppm error). UV/vis (toluene): λ 402 (ϵ = 33259), 422 (ϵ = 164714), 515 (ϵ = 8578), 545 (ϵ = 2507), 587 (ϵ = 2639).

2HPOP

2HPOBr (10 mg, 0.0080 mmol), pinacol pyreneboronate (**1**) (23.3 mg, 0.071 mmol), [PdCl₂(dppf)] (9.3 mg, 0.0128 mmol) and ^tBuONa (18.5 mg, 0.192 mmol) were mixed in a sealed vessel specifically designed for microwave irradiation and put the microwave reactor inside a two-necked round-bottom flask in order to keep the system under an inert atmosphere. 1.4 ml of dry toluene was added. The mixture was stirred inside a microwave reactor at 150 °C for 135 min (the pressure reached up to 3.8 bar). After cooling, the solvent was removed under vacuum and the crude was purified by column chromatography on silica gel,

using hexane/AcOEt gradient elution (3:1– 2:1 – 1:1) and CHCl_3 to finally give a purple solid **2HPOP** (5.0 mg, 28% yield). ^1H NMR (500 MHz, Chloroform-*d*) δ : 9.46 (s, 8H, H_2), 8.85 (d, $J = 9.3$ Hz, 8H, H_{10}), 8.73 (d, $J = 1.7$ Hz, 8H, H_6), 8.46 (d, $J = 7.9$ Hz, 8H, H_{18}), 8.42 (t, $J = 1.7$ Hz, 4H, H_8), 8.31 (d, $J = 7.9$ Hz, 8H, H_{17}), 8.19 – 8.15 (m, 16H, $\text{H}_{14}+\text{H}_{11}$), 8.12 – 8.07 (m, 16H, $\text{H}_{13}+\text{H}_{12}$), 8.05 (d, $J = 7.7$ Hz, 8H, H_{16}), 7.94 (t, $J = 7.7$ Hz, 8H, H_{15}), -2.50 (br, 2H, H_1). $^{13}\text{C}\{^1\text{H}\}$ NMR (126 MHz, Chloroform-*d*) δ : 142.4 (C_5), 139.8 (C_{19}), 136.9 (C_7), 136.0 (C_6), 132.2 (C_8), 131.4 (C_{22}), 130.8 ($\text{C}_{24}+\text{C}_{20}$), 128.7 (C_9), 128.1 (C_{18}), 127.9 (C_{11}), 127.5 (C_{13}), 127.3 (C_{12}), 125.9 (C_{15}), 125.1 (C_{14}), 125.05 (C_{10}), 125.01 (C_q), 124.9 (C_{16}), 124.82 (C_{17}), 124.80 (C_q), 120.1 (C_4). HRMS (MALDI-TOF) m/z : $[\text{M}+\text{H}]^+$ Calcd for $\text{C}_{172}\text{H}_{94}\text{N}_4$ 2214.7473; Found 2214.7424 (-4.9 ppm error). UV/vis (toluene): λ 280 ($\epsilon = 275508$), 350 ($\epsilon = 238277$), 410 ($\epsilon = 106537$), 428 ($\epsilon = 503476$), 518 ($\epsilon = 25202$), 551 ($\epsilon = 12601$).

ZnPOP

2HPOP (5.0 mg, 0.0022 mmol) and $\text{Zn}(\text{AcO})_2 \cdot 2\text{H}_2\text{O}$ (7.2 mg, 0.033 mmol) were mixed in a sealed vessel specifically designed for microwave irradiation and a mixture of 1.5 ml of CHCl_3 /1.5 ml of toluene was added. The mixture was stirred inside a microwave reactor at 120 °C for 90 min (the pressure reached up to 4.7 bar). After cooling, the solvent was removed under vacuum and the solid obtained was dissolved in 10 ml of CHCl_3 and placed into a separatory funnel and washed with 5 ml of H_2O . The organic layer was removed under low pressure to give a purple solid **ZnPOP** (4.5 mg, 91%). ^1H NMR (500 MHz, Chloroform-*d*) δ : 9.56 (s, 8H, H_2), 8.85 (d, $J = 9.5$ Hz, 8H, H_{10}), 8.71 (d, $J = 0.7$ Hz, 8H, H_6), 8.45 (d, $J = 8.0$ Hz, 8H, H_{18}), 8.40 (t, $J = 0.7$ Hz, 4H, H_8), 8.28 (d, $J = 8.0$ Hz, 8H, H_{17}), 8.17– 8.12 (m, 16H, $\text{H}_{14}+\text{H}_{11}$), 8.11 – 8.04 (m, 16H, $\text{H}_{13}+\text{H}_{12}$), 7.99 (br, 8H, H_{16}), 7.90 (br, 8H, H_{15}). $^{13}\text{C}\{^1\text{H}\}$ NMR (126 MHz, Chloroform-*d*) δ : 150.3 (C_3), 143.2 (C_5), 139.5 (C_{19}), 137.1 (C_7), 136.0 (C_6), 132.3 (C_2), 131.8 (C_8), 131.2 (C_{22}), 130.7 ($\text{C}_{24}+\text{C}_{20}$), 128.7 (C_9), 128.0 (C_{18}), 127.7 (C_{11}), 127.4 (C_{13}), 127.2 (C_{12}), 125.7 (C_{15}), 124.97 (C_{14}), 124.93 (C_{10}), 124.8 (C_{16}), 124.6 (C_{17}), 120.8 (C_4). HRMS (MALDI-TOF) m/z : $[\text{M}+\text{H}]^+$ calcd for $\text{C}_{172}\text{H}_{92}\text{N}_4\text{Zn}$ 2277.6652; Found: 2277.668 (1.5 ppm error). UV/vis (toluene): λ 280 ($\epsilon = 274000$), 350 ($\epsilon = 208000$), 415 ($\epsilon = 81000$), 432 ($\epsilon = 442000$), 551 ($\epsilon = 23000$).

ZnPOBr

2HPOBr (60 mg, 0.048 mmol) and $\text{Zn}(\text{AcO})_2 \cdot 2\text{H}_2\text{O}$ (84 mg, 0.382 mmol) were mixed in a sealed vessel specifically designed for microwave irradiation, and 1.5 ml of CHCl_3 was added. The mixture was stirred inside the microwave reactor at 150 °C for 150 min; the pressure reached up to 10 bar. Subsequently, the crude was dissolved in 20 ml of CHCl_3 , placed in a separatory funnel, and washed with 10 ml of H_2O . The organic layer was removed under low pressure to give the purple solid **ZnPOBr** (56 mg, 89% yield). ^1H NMR (500 MHz, Chloroform-*d*) δ : 8.99 (s, 8H, H_2), 8.31 (d, $J = 1.8$ Hz, 8H, H_6), 8.15 (t, $J = 1.8$ Hz, 4H, H_8). $^{13}\text{C}\{^1\text{H}\}$ NMR (126 MHz, Chloroform-*d*) δ : 149.9 (C_3), 135.8 (C_6), 133.7 (C_8), 132.3 (C_2), 121.4 (C_7 -in), 118.4 (C_4 -in). HRMS (MALDI-TOF) m/z : $[\text{M}+\text{H}]^+$ Calcd for $\text{C}_{44}\text{H}_{20}\text{Br}_8\text{N}_4\text{Zn}$ 1309.4344; Found: 1309.4372 (2.1 ppm error). UV/vis (toluene): λ 401 ($\epsilon = 24400$), 424 ($\epsilon = 160981$), 515 ($\epsilon = 6428$), 550 ($\epsilon = 6100$), 587 ($\epsilon = 2529$).

ZnPOB

ZnPOBr (30 mg, 0.023 mmol), bis(pinacolato)diboron (70 mg, 0.276 mmol), [PdCl₂(dppf)] (6.7 mg, 0.0092 mmol), and AcOK (54.16 mg, 0.552 mmol) were mixed in a sealed vessel specifically designed for microwave irradiation. The microwave Vessel was placed inside a two-necked round-bottom flask in order to keep the system under an inert atmosphere. 0.7 ml of dry dioxane and 35 μ l of pyridine were then added to the microwave vessel. The mixture was stirred inside the microwave reactor at 160 °C for 150 min; the pressure reached 3 bar. Subsequently, the solvent was removed under vacuum and the obtained solid was dissolved in 20 ml of CHCl₃, placed in a separatory funnel, and washed with 10 ml of H₂O. The solvent was evaporated from the deep red organic layer, and the obtained solid was transferred to a centrifugation vial and underwent five wash-centrifuge cycles with hexane to finally afford the purple solid **ZnPOB** (27 mg, 71% yield). ¹H NMR (500 MHz, Chloroform-*d*): δ 8.85 (s, 8H, H₂), 8.73 (d, *J* = 1.2 Hz, 8H, H₆), 8.64 (t, *J* = 1.2 Hz, 4H, H₈), 1.36 (s, 96H, H₁₀). ¹³C{¹H} NMR (126 MHz, Chloroform-*d*): δ 150.2 (C₃), 142.8 (C₆), 141.7 (C₅), 140.0 (C₈), 132.0 (C₂), 126.2 (C₇), 120.9 (C₄), 83.8 (C₉), 24.9 (C₁₀). HRMS (MALDI-TOF) *m/z*: [M+H]⁺ Calcd for C₉₂H₁₁₆B₈N₄O₁₆Zn 1683.8502; Found 1683.8619 (11.7 ppm error). UV/vis (toluene): λ 405 (ϵ = 22741), 426 (ϵ = 186524), 550 (ϵ = 12414).

2HPOB

2HPOBr (20 mg, 0.016 mmol), bis(pinacolato)diboron (48.75 mg, 0.192 mmol), [PdCl₂(dppf)] (4.68 mg, 0.0064 mmol), and AcOK (36.9 mg, 0.384 mmol) were mixed into a sealed vessel specifically designed for microwave irradiation. The microwave vessel was placed inside a two-necked round-bottom flask in order to keep the system under an inert atmosphere. 0.5 ml of dry dioxane was then added to the microwave vessel. The mixture was stirred inside the microwave reactor at 160 °C for 150 min and reached a pressure of 3 bar. Subsequently, the solvent was removed under vacuum and the obtained solid was dissolved in 15 ml of CHCl₃, placed in a separatory funnel, and washed with 8 ml of H₂O. The solvent of the deep red organic layer was evaporated. The obtained solid was transferred to a centrifugation vial and underwent five washing-centrifugation cycles with hexane (5 times) to finally afford the purple solid **2HPOB** (19 mg, 73% yield). ¹H NMR (500 MHz, Chloroform-*d*): δ 8.76 (s, 8H, H₂), 8.71 (d, *J* = 1.2 Hz, 8H, H₆), 8.65 (t, *J* = 1.2 Hz, 4H, H₈), 1.36 (s, 96H, H₁₀), -2.79 (br, 2H, H₁). ¹³C{¹H} NMR (126 MHz, Chloroform-*d*): δ 142.8 (C₆), 141.0 (C₅), 140.3 (C₈), 131.3 (C₂), 126.4 (C₇), 120.0 (C₄), 83.9 (C₉), 24.9 (C₁₀). HRMS (MALDI-TOF) *m/z*: [M+H]⁺ Calcd for C₉₂H₁₁₈B₈N₄O₁₆ 1622.9443; Found: 1622.9426 (-1.7 ppm error). UV/vis (toluene): λ 407 (ϵ = 59125), 422 (ϵ = 298419), 515 (ϵ = 12104), 548 (ϵ = 3957).

ASSOCIATED CONTENT

Supporting Information

The Supporting Information is available free of charge on the ACS Publications website. Spectra of compounds are provided in PDF format.

AUTHOR INFORMATION

Corresponding Author

Celedonio M. Álvarez: GIR MIOMeT, IU CINQUIMA/Química Inorgánica, Facultad de Ciencias, Universidad de Valladolid, E47011, Valladolid, Spain.

E-mail: celedonio.alvarez@uva.es

Raul Garcia-Rodriguez GIR MIOMeT, IU CINQUIMA/Química Inorgánica, Facultad de Ciencias, Universidad de Valladolid, E47011, Valladolid, Spain.

E-mail: raul.garcia.rodriguez@uva.es

Notes

The authors declare no competing financial interests.

ACKNOWLEDGMENT

This research was supported by the Spanish Ministerio de Economía y Competitividad (MINECO) (project number CTQ 2013-41067-P).

R.G.-R. acknowledges the Spanish MINECO – AEI and the European Union (ESF) for a Ramon y Cajal contract (RYC-2015–19035). H.

B. acknowledges the Alfonso Martín Escudero Foundation for a postdoctoral fellowship.

REFERENCES

- (1) Pérez, E. M.; Martín, N. π - π Interactions in Carbon Nanostructures. *Chem. Soc. Rev.* **2015**, *44*, 6425-6433.
- (2) Pérez, E. M.; Martín, N. Curves Ahead: Molecular Receptors for Fullerenes Based on Concave-Convex Complementarity. *Chem. Soc. Rev.* **2008**, *37*, 1512-1519.
- (3) (a) Scott, L. T.; Hashemi, M. M.; Bratcher, M. S. Corannulene Bowl-to-Bowl Inversion Is Rapid at Room Temperature. *J. Am. Chem. Soc.* **1992**, *114*, 1920-1921. (b) Wu, Y.-T.; Siegel, J. S. Aromatic Molecular-Bowl Hydrocarbons: Synthetic Derivatives, Their Structures, and Physical Properties. *Chem. Rev.* **2006**, *106*, 4843-4867. (c) Li, X.; Kang, F.; Inagaki, M. Buckybowls: Corannulene and Its Derivatives. *Small* **2016**, *12*, 3206-3223. (d) Saito, M.; Shinokubo, H.; Sakurai, H. Figuration of Bowl-Shaped π -Conjugated Molecules: Properties and Functions. *Materials Chemistry Frontiers* **2018**, *2*, 635-661. (e) Nestoros, E.; Stuparu, M. C. Corannulene: A Molecular Bowl of Carbon with Multifaceted Properties and Diverse Applications. *Chem. Commun.* **2018**, *54*, 6503-6519.
- (4) (a) Ehli, C.; Rahman, G. M. A.; Jux, N.; Balbinot, D.; Guldi, D. M.; Paolucci, F.; Marcaccio, M.; Paolucci, D.; Melle-Franco, M.; Zerbetto, F.; Campidelli, S.; Prato, M. Interactions in Single Wall Carbon Nanotubes/Pyrene/Porphyrin Nanohybrids. *J. Am. Chem. Soc.* **2006**, *128*, 11222-11231. (b) Zhao, Y.-L.; Hu, L.; Grüner, G.; Stoddart, J. F. A Tunable Photosensor. *J. Am. Chem. Soc.* **2008**, *130*, 16996-17003. (c) Zhao, Y.-L.; Stoddart, J. F. Noncovalent Functionalization of Single-Walled Carbon Nanotubes. *Acc. Chem. Res.* **2009**, *42*, 1161-1171. (d) Bilalis, P.; Katsigiannopoulos, D.; Avgeropoulos, A.; Sakellariou, G. Non-covalent Functionalization of Carbon Nanotubes with Polymers. *RSC Advances* **2014**, *4*, 2911-2934. (e) de Juan, A.; López-Moreno, A.; Calbo, J.; Ortí, E.; Pérez, E. M. Determination of Association Constants towards Carbon Nanotubes. *Chem. Sci.* **2015**, *6*, 7008-7014. (f) López-Moreno, A.; Pérez, E. M. Pyrene-based Mechanically Interlocked SWNTs. *Chem. Commun.* **2015**, *51*, 5421-5424. (g) Calbo, J.; López-Moreno, A.; de Juan, A.; Comer, J.; Ortí,

E.; Pérez, E. M. Understanding Noncovalent Interactions of Small Molecules with Carbon Nanotubes. *Chemistry – A European Journal* **2017**, *23*, 12909-12916.

(5) (a) Zhang, M.; Parajuli, R. R.; Mastrogiovanni, D.; Dai, B.; Lo, P.; Cheung, W.; Brukh, R.; Chiu, P. L.; Zhou, T.; Liu, Z.; Garfunkel, E.; He, H. Production of Graphene Sheets by Direct Dispersion with Aromatic Healing Agents. *Small* **2010**, *6*, 1100-1107. (b) Mann, J. A.; Rodríguez-López, J.; Abruña, H. D.; Dichtel, W. R. Multivalent Binding Motifs for the Noncovalent Functionalization of Graphene. *J. Am. Chem. Soc.* **2011**, *133*, 17614-17617. (c) Ciesielski, A.; Samori, P. Graphene via Sonication Assisted Liquid-Phase Exfoliation. *Chem. Soc. Rev.* **2014**, *43*, 381-398. (d) KC, C. B.; Lim, G. N.; D'Souza, F. Charge Separation in Graphene-Decorated Multimodular Tris(pyrene)-Subphthalocyanine-Fullerene Donor-Acceptor Hybrids. *Angew. Chem. Int. Ed.* **2015**, *54*, 5088-5092. (e) Ciesielski, A.; Samori, P. Supramolecular Approaches to Graphene: From Self-Assembly to Molecule-Assisted Liquid-Phase Exfoliation. *Adv. Mater.* **2016**, *28*, 6030-6051. (f) Bottari, G.; Herranz, M. Á.; Wibmer, L.; Volland, M.; Rodríguez-Pérez, L.; Guldi, D. M.; Hirsch, A.; Martín, N.; D'Souza, F.; Torres, T. Chemical Functionalization and Characterization of Graphene-Based Materials. *Chem. Soc. Rev.* **2017**, *46*, 4464-4500. (g) Garrido, M.; Calbo, J.; Rodríguez-Pérez, L.; Aragó, J.; Ortí, E.; Herranz, M. A.; Martín, N. Non-covalent Graphene Nanobuds from Mono- and Tripodal Binding Motifs. *Chem. Commun.* **2017**, *53*, 12402-12405.

(6) Mulla, K.; Shaik, H.; Thompson, D. W.; Zhao, Y. TTFV-Based Molecular Tweezers and Macrocycles as Receptors for Fullerenes. *Org. Lett.* **2013**, *15*, 4532-4535.

(7) (a) Ronson, T. K.; League, A. B.; Gagliardi, L.; Cramer, C. J.; Nitschke, J. R. Pyrene-Edged Fe^{II}₄L₆ Cages Adaptively Reconfigure during Guest Binding. *J. Am. Chem. Soc.* **2014**, *136*, 15615-15624. (b) Ronson, T. K.; Meng, W.; Nitschke, J. R. Design Principles for the Optimization of Guest Binding in Aromatic-Paneled Fe^{II}₄L₆ Cages. *J. Am. Chem. Soc.* **2017**, *139*, 9698-9707.

(8) (a) Álvarez, C. M.; García-Escudero, L. A.; García-Rodríguez, R.; Martín-Álvarez, J. M.; Miguel, D.; Rayón, V. M. Enhanced Association for C₇₀ over C₆₀ with a Metal Complex with Corannulene Derivate Ligands. *Dalton Transactions* **2014**, *43*, 15693-15696. (b) Abeyratne Kuragama, P. L.; Fronczek, F. R.; Sygula, A. Bis-corannulene Receptors for Fullerenes Based on Klärner's Tethers: Reaching the Affinity Limits. *Org. Lett.* **2015**, *17*, 5292-5295. (c) Yang, D.-C.; Li, M.; Chen, C.-F. A Bis-corannulene Based Molecular Tweezer with Highly Sensitive and Selective Complexation of C₇₀ over C₆₀. *Chem. Commun.* **2017**, *53*, 9336-9339.

(9) (a) Sygula, A.; Fronczek, F. R.; Sygula, R.; Rabideau, P. W.; Olmstead, M. M. A Double Concave Hydrocarbon Buckycatcher. *J. Am. Chem. Soc.* **2007**, *129*, 3842-3843. (b) Stuparu, M. C. Rationally Designed Polymer Hosts of Fullerene. *Angew. Chem. Int. Ed.* **2013**, *52*, 7786-7790. (c) Le, V. H.; Yanney, M.; McGuire, M.; Sygula, A.; Lewis, E. A. Thermodynamics of Host-Guest Interactions between Fullerenes and a Buckycatcher. *J. Phys. Chem. B.* **2014**, *118*, 11956-11964. (d) Yanney, M.; Fronczek, F. R.; Sygula, A. A 2:1 Receptor/C₆₀ Complex as a Nanosized Universal Joint. *Angew. Chem. Int. Ed.* **2015**, *54*, 11153-11156. (e) Kumarasinghe, K. G. U. R.; Fronczek, F. R.; Valle, H. U.; Sygula, A. Bis-corannulenoanthracene: An Angularly Fused Pentacene as a Precursor for Barrelene-Tethered Receptors for Fullerenes. *Org. Lett.* **2016**, *18*, 3054-3057. (f) Barbero, H.; Ferrero, S.; Álvarez-Miguel, L.; Gómez-Iglesias, P.; Miguel, D.; Álvarez, C. M. Affinity Modulation of Photoresponsive Hosts for Fullerenes: Light-Gated Corannulene Tweezers. *Chem. Commun.* **2016**, *52*, 12964-12967.

(10) (a) Boyd, P. D. W.; Hodgson, M. C.; Rickard, C. E. F.; Oliver, A. G.; Chaker, L.; Brothers, P. J.; Bolskar, R. D.; Tham, F. S.; Reed, C. A. Selective Supramolecular Porphyrin/Fullerene Interactions. *J. Am. Chem. Soc.* **1999**, *121*, 10487-10495. (b) Olmstead, M. M.; Costa,

D. A.; Maitra, K.; Noll, B. C.; Phillips, S. L.; Van Calcar, P. M.; Balch, A. L. Interaction of Curved and Flat Molecular Surfaces. The Structures of Crystalline Compounds Composed of Fullerene (C₆₀, C₆₀O, C₇₀, and C₁₂₀O) and Metal Octaethylporphyrin Units. *J. Am. Chem. Soc.* **1999**, *121*, 7090-7097. (c) Boyd, P. D. W.; Reed, C. A. Fullerene–Porphyrin Constructs. *Acc. Chem. Res.* **2005**, *38*, 235-242. (d) Bhyrappa, P.; Karunanithi, K. Porphyrin–Fullerene, C₆₀, Cocrystallates: Influence of C₆₀ on the Porphyrin Ring Conformation. *Inorg. Chem.* **2010**, *49*, 8389-8400. (e) Bhyrappa, P.; Sarangi, U. K.; Varghese, B. Switching the Macrocyclic Conformation from Nonplanar to Planar in Cobalt(II) and Copper(II) β-Tetra-2'-thienyl-meso-tetraphenylporphyrin Cocrystallates with C₆₀. *Eur. J. Inorg. Chem.* **2014**, *2014*, 5646-5650.

(11) (a) Tashiro, K.; Aida, T. Metalloporphyrin Hosts for Supramolecular Chemistry of Fullerenes. *Chem. Soc. Rev.* **2007**, *36*, 189-197. (b) Bromby, A. D.; Hogan, D. T.; Sutherland, T. C. Core Expanded, 21,23-Dithiadiazacene[1,2-c]porphyrin Interactions with [60]Fullerene. *New J. Chem.* **2017**, *41*, 4802-4805.

(12) Durot, S.; Taesch, J.; Heitz, V. Multiporphyrinic Cages: Architectures and Functions. *Chem. Rev.* **2014**, *114*, 8542-8578.

(13) (a) Canevet, D.; Pérez, E. M.; Martín, N. Wraparound Hosts for Fullerenes: Tailored Macrocycles and Cages. *Angew. Chem. Int. Ed.* **2011**, *50*, 9248-9259. (b) Jurow, M.; Farley, C.; Pabon, C.; Hageman, B.; Dolor, A.; Drain, C. M. Facile Synthesis of a Flexible Tethered Porphyrin Dimer That Preferentially Complexes Fullerene C₇₀. *Chem. Commun.* **2012**, *48*, 4731-4733. (c) García-Simón, C.; Garcia-Borràs, M.; Gómez, L.; Parella, T.; Osuna, S.; Juanhuix, J.; Imaz, I.; Maspocho, D.; Costas, M.; Ribas, X. Sponge-like Molecular Cage for Purification of Fullerenes. *Nature Communications* **2014**, *5*, 5557. (d) Fang, X.; Zhu, Y.-Z.; Zheng, J.-Y. Clawlike Tripodal Porphyrin Trimer: Ion-Controlled On–Off Fullerene Binding. *J. Org. Chem.* **2014**, *79*, 1184-1191. (e) García-Simón, C.; Costas, M.; Ribas, X. Metallosupramolecular Receptors for Fullerene Binding and Release. *Chem. Soc. Rev.* **2016**, *45*, 40-62.

(14) Álvarez, C. M.; Barbero, H.; Ferrero, S.; Miguel, D. Synergistic Effect of Tetraaryl Porphyrins Containing Corannulene and Other Polycyclic Aromatic Fragments as Hosts for Fullerenes. Impact of C₆₀ in a Statistically Distributed Mixture of Atropisomers. *J. Org. Chem.* **2016**, *81*, 6081-6086.

(15) (a) Kimura, M.; Shiba, T.; Muto, T.; Hanabusa, K.; Shirai, H. Intramolecular Energy Transfer in 1,3,5-Phenylene-Based Dendritic Porphyrins. *Macromolecules* **1999**, *32*, 8237-8239. (b) Kimura, M.; Shiba, T.; Yamazaki, M.; Hanabusa, K.; Shirai, H.; Kobayashi, N. Construction of Regulated Nanospace around a Porphyrin Core. *J. Am. Chem. Soc.* **2001**, *123*, 5636-5642.

(16) Kappe, C. O. Controlled Microwave Heating in Modern Organic Synthesis. *Angew. Chem. Int. Ed.* **2004**, *43*, 6250-6284.

(17) Yao, D.; Zhang, X.; Mongin, O.; Paul, F.; Paul-Roth, C. O. Synthesis and Characterization of New Conjugated Fluorenyl-Porphyrin Dendrimers for Optics. *Chemistry – A European Journal* **2016**, *22*, 5583-5597.

(18) (a) Lemon, C. M.; Brothers, P. J.; Boitrel, B. Porphyrin Complexes of the Period 6 Main Group and Late Transition Metals. *Dalton Transactions* **2011**, *40*, 6591-6609. (b) Kadish, K. M.; Smith, K. M.; Guillard, R. *Handbook of Porphyrin Science (Volumes 21- 25)*; World Scientific Publishing Company, 2012; Vol. Volumes 21 – 25. (c) Valicsek, Z.; Horváth, O. Application of the Electronic Spectra of Porphyrins for Analytical Purposes: The Effects of Metal Ions and Structural Distortions. *Microchem. J.* **2013**, *107*, 47-62. (d) Senge, M. O.; MacGowan, S. A.; O'Brien, J. M. Conformational Control of Cofactors in Nature - The Influence of Protein-Induced Macrocyclic Distortion on the Biological Function of Tetrapyrroles. *Chem. Commun.* **2015**, *51*, 17031-17063.

- (19) (a) Jian-Yu, Z.; Kentaro, T.; Yusuke, H.; Kazushi, K.; Kazuhiko, S.; Takuzo, A.; Shigeru, S.; Kentaro, Y. Cyclic Dimers of Metalloporphyrins as Tunable Hosts for Fullerenes: A Remarkable Effect of Rhodium(III). *Angew. Chem. Int. Ed.* **2001**, *40*, 1857-1861. (b) Sun, D.; Tham, F. S.; Reed, C. A.; Chaker, L.; Boyd, P. D. W. Supramolecular Fullerene-Porphyrin Chemistry. Fullerene Complexation by Metalated "Jaws Porphyrin" Hosts. *J. Am. Chem. Soc.* **2002**, *124*, 6604-6612. (c) Wang, Y.-B.; Lin, Z. Supramolecular Interactions between Fullerenes and Porphyrins. *J. Am. Chem. Soc.* **2003**, *125*, 6072-6073. (d) Ayako, O.; Kentaro, T.; Kentaro, Y.; Takahiro, T.; Takeshi, A.; Takuzo, A. A Self-Regulatory Host in an Oscillatory Guest Motion: Complexation of Fullerenes with a Short-Spaced Cyclic Dimer of an Organorhodium Porphyrin. *Angew. Chem. Int. Ed.* **2006**, *45*, 3542-3546. (e) Yanagisawa, M.; Tashiro, K.; Yamasaki, M.; Aida, T. Hosting Fullerenes by Dynamic Bond Formation with an Iridium Porphyrin Cyclic Dimer: A "Chemical Friction" for Rotary Guest Motions. *J. Am. Chem. Soc.* **2007**, *129*, 11912-11913.
- (20) (a) A. Shelnutt, J.; Song, X.-Z.; Ma, J.-G.; Jia, S.-L.; Jentzen, W.; J. Medforth, C.; J. Medforth, C. Nonplanar Porphyrins and Their Significance in Proteins. *Chem. Soc. Rev.* **1998**, *27*, 31-42. (b) Haddad, R. E.; Gazeau, S.; Pécaut, J.; Marchon, J.-C.; Medforth, C. J.; Shelnutt, J. A. Origin of the Red Shifts in the Optical Absorption Bands of Nonplanar Tetraalkylporphyrins. *J. Am. Chem. Soc.* **2003**, *125*, 1253-1268. (c) Senge, M. O. Exercises in Molecular Gymnastics-Bending, Stretching and Twisting Porphyrins. *Chem. Commun.* **2006**, *0*, 243-256.
- (21) (a) Hunter, C. A.; Sanders, J. K. M. The Nature of π - π . Interactions. *J. Am. Chem. Soc.* **1990**, *112*, 5525-5534. (b) Saegusa, Y.; Ishizuka, T.; Kojima, T.; Mori, S.; Kawano, M.; Kojima, T. Supramolecular Interaction of Fullerenes with a Curved π -Surface of a Monomeric Quadruply Ring-Fused Porphyrin. *Chemistry – A European Journal* **2015**, *21*, 5302-5306.
- (22) Thordarson, P. In *Supramolecular Chemistry: From Molecules to Nanomaterials*; Gale, P. A., Steed, J. W., Eds.; John Wiley & Sons: Chichester, UK, 2012; Vol. 2, p 239-274.
- (23) (a) Thordarson, P. Determining Association Constants from Titration Experiments in Supramolecular Chemistry. *Chem. Soc. Rev.* **2011**, *40*, 1305-1323. (b) Brynn Hibbert, D.; Thordarson, P. The Death of the Job Plot, Transparency, Open Science and Online Tools, Uncertainty Estimation Methods and Other Developments in Supramolecular Chemistry Data Analysis. *Chem. Commun.* **2016**, *52*, 12792-12805.
- (24) (a) Yanney, M.; Sygula, A. Tridental Molecular Clip with Corannulene Pincers: Is Three Better Than Two? *Tetrahedron Lett.* **2013**, *54*, 2604-2607. (b) Álvarez, C. M.; Aullón, G.; Barbero, H.; García-Escudero, L. A.; Martínez-Pérez, C.; Martín-Álvarez, J. M.; Miguel, D. Assembling Nonplanar Polyaromatic Units by Click Chemistry. Study of Multicorannulene Systems as Host for Fullerenes. *Org. Lett.* **2015**, *17*, 2578-2581.
- (25) (a) Taylor, R.; Hare, J. P.; Abdul-Sada, A. a. K.; Kroto, H. W. Isolation, Separation and Characterisation of the Fullerenes C₆₀ and C₇₀: The Third Form of Carbon. *J. Chem. Soc., Chem. Commun.* **1990**, *0*, 1423-1425. (b) Ajie, H.; Alvarez, M. M.; Anz, S. J.; Beck, R. D.; Diederich, F.; Fostiropoulos, K.; Huffman, D. R.; Kraetschmer, W.; Rubin, Y.; et al. Characterization of the Soluble All-Carbon Molecules C₆₀ and C₇₀. *The Journal of Physical Chemistry* **1990**, *94*, 8630-8633. (c) Diederich, F.; Whetten, R. L. Beyond C₆₀: The Higher Fullerenes. *Acc. Chem. Res.* **1992**, *25*, 119-126.
- (26) Hare, J. P.; Kroto, H. W.; Taylor, R. Reprint of: Preparation and UV/visible Spectra of Fullerenes C₆₀ and C₇₀. *Chem. Phys. Lett.* **2013**, *589*, 57-60.

(27) (a) Zhang, C.; Wang, Q.; Long, H.; Zhang, W. A highly C₇₀ selective shape-persistent rectangular prism constructed through one-step alkyne metathesis. *J. Am. Chem. Soc.* **2011**, *133*, 20995-21001. (b) Shi, Y.; Cai, K.; Xiao, H.; Liu, Z.; Zhou, J.; Shen, D.; Qiu, Y.; Guo, Q. H.; Stern, C.; Wasielewski, M. R.; Diederich, F.; Goddard, W. A., Stoddart, J. F. Selective Extraction of C₇₀ by a Tetragonal Prismatic Porphyrin Cage. *J. Am. Chem. Soc.* **2018**, *140*, 13835-13842.

(28) (a) Armarego, W. L. F.; Chai, C. L. L. *Purification of Laboratory Chemicals, 6th*; Butterworth-Heinemann: London, 2009. (b) Williams, D. B. G.; Lawton, M. Drying of Organic Solvents: Quantitative Evaluation of the Efficiency of Several Desiccants. *J. Org. Chem.* **2010**, *75*, 8351-8354.

(29) Matthias, B.; Wilfried, W.; Martin, J.; Wolfgang, R.; Claudia, M.; Irene, B.; Hans, H.; A. Dieter, S. Synthesis and Spectroscopic Properties of Arene-Substituted Pyrene Derivatives as Model Compounds for Fluorescent Polarity Probes. *Eur. J. Org. Chem.* **2001**, *2001*, 3819-3829.

Table of Contents artwork

